

Algebraic Bethe Ansatz for the FPL² model

J. Jacobsen and P. Zinn-Justin

Laboratoire de Physique Théorique et Modèles Statistiques

Université Paris-Sud, Bâtiment 100

F-91405 Orsay Cedex, France

An exact solution of the model of fully packed loops of two colors on a square lattice has recently been proposed by Dei Cont and Nienhuis using the coordinate Bethe Ansatz approach. We point out here a simpler alternative, in which the transfer matrix is directly identified as a product of R-matrices; this allows to apply the (nested) algebraic Bethe Ansatz, which leads to the same Bethe equations. We comment on some of the applications of this result.

1. Introduction

Models of fluctuating loops play a key role in two-dimensional statistical physics, and a range of well-known models (Ising, Potts, percolation, $O(n)$, to name but a few) can be conveniently studied through their reformulations as loop models. Exact results about loop models have been produced by a variety of techniques, including the Coulomb gas, conformal field theory, the Bethe Ansatz, and stochastic Loewner evolution.

In this note we study the fully packed two-color loop model on the square lattice (henceforth referred to as the FPL^2 model) from the point of view of the algebraic Bethe Ansatz. The FPL^2 model was introduced in [1] as a generalization of the four-coloring model of the square lattice edges [2]. It is defined by assigning one of two colors (black or white) to each lattice edge, subject to the constraint that every vertex be incident to two black and two white edges. In this way, the black and white edges form fully packed loops which are given fugacities n_b and n_w depending on their color.

The FPL^2 model has attracted much interest over the last decade. Successive advances in the Coulomb gas technique have permitted to compute the central charge and the critical exponents for a number of special cases: the four-coloring model $(n_b, n_w) = (2, 2)$ [2,1], the dimer-loop model $(n_b, n_w) = (2, 1)$ [3], and the equal-fugacity case $n_b = n_w$ [4]. This eventually led to the solution for general values of n_b and n_w [5]. An interesting special case is that of Hamiltonian walks, with $(n_b, n_w) = (0, 1)$ [6]. A generalization of the FPL^2 model, obtained by giving the loops a bending rigidity, was solved in [7]. It contains as a special case the so-called Flory model of protein melting [8].

All these Coulomb gas results are obtained by making certain reasonable, but non-rigorous, assumptions about the long wavelength behavior of an associated interface model. The resulting critical exponents are however believed to be exact, and they have been successfully tested against numerical Monte Carlo [1,3] and transfer matrix [9,6,7] results.

To give the results obtained by the Coulomb gas a rigorous status, and to go beyond it and derive results which are not obtainable from a continuum approach, it is natural to turn to the methods of integrability. Following earlier work on the four-coloring model [10], Dei Cont and Nienhuis [11] have very recently succeeded in finding a coordinate Bethe Ansatz for the equal-fugacity FPL^2 model. In particular they have computed the exact partition function. Moreover, they have shown that when $n_b \neq n_w$, the FPL^2 model is not integrable, in agreement with earlier expectations [6].

However the Coordinate Bethe Ansatz is a rather complex technique, which, in order to be made fully rigorous, would require investigation of a large number of specific configurations. The goal of the present note is to present a simpler alternative, in which the transfer matrix of the equal-fugacity FPL² model (henceforth we note $n \equiv n_b = n_w$) is identified with a product of trigonometric R-matrices of $U_q(\widehat{sl(4)})$ with $n = -q - q^{-1}$ (and an appropriate twist). Applying the (nested) algebraic Bethe Ansatz allows us to recover the Bethe equations of Ref. [11] in a straightforward fashion. As a bonus we obtain the central charge and the critical exponents, which are found to agree with the non-rigorous results of Ref. [6]. We also comment on a $n \rightarrow -n$ symmetry of some of the sectors of the transfer matrix.

The paper is organized as follows. The FPL² model is defined in Sec. 2. In Sec. 3 we define its transfer matrix in terms of an R-matrix that adds four vertices and a twist matrix that takes care of the boundary conditions. We then show how these matrices are related to those of the affine quantum group $U_q(\widehat{sl(4)})$ with alternating fundamental and conjugate representations. The corresponding Bethe Ansatz equations are discussed in Sec. 4, and we reproduce in particular the eigenvalues of the transfer matrix [11]. Finally, in Sec. 5, we give the expressions of the central charge and conformal weights for $n \leq 2$, and we compare our results to those obtained for fully packed loops on the hexagonal lattice.

2. The FPL² model

Following [6], we reformulate the FPL² model as a 24-vertex model. For each vertex of the square lattice, the four incident edges are decorated with arrows of two possible orientations (outgoing or ingoing with respect to the vertex) and two possible colors (black or white), subject to the constraint that each of the four possibilities be represented exactly once around every vertex. Clearly, following the arrows of a given color traces out an oriented loop of that color. Note that reversing the arrows along any one loop, and leaving all other arrows unchanged, leads to another allowed configuration.

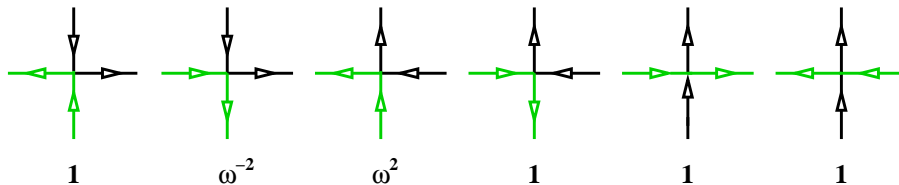


Fig. 1: The six types of vertices in the 24-vertex model (the remaining vertices are obtained by $\pi/2$ rotations) with their corresponding weights.

We then assign a weight $w = w_b w_w$ to each vertex which is the product of weights w_b and w_w coming from the oriented black and white loops respectively. The black weight $w_b = \omega$ (resp. $w_b = \omega^{-1}$) when the black loop makes a right turn (resp. a left turn) at the concerned vertex, and $w_b = 1$ when the black loop goes straight. For the white weight we choose the opposite convention, that is with ω and ω^{-1} exchanged. The weights of the six types of vertices which are unrelated by $\pi/2$ rotations are given in Fig. 1.

The FPL² model with fugacity n for both colors of loops is recovered by summing independently over the orientations of all loops (black and white). An anticlockwise (resp. clockwise) black loop contributes ω^4 (resp. ω^{-4}) to the fugacity, as it must turn four times more (resp. less) to the left than to the right. Thus, ω is fixed by

$$n = \omega^4 + \omega^{-4}. \quad (2.1)$$

In order to apply the Bethe Ansatz it is important to specify the boundary conditions. In the following we shall specialize to the case where the square lattice is wrapped on a cylinder, i.e., with periodic boundary conditions across a horizontal row of $2L$ vertices [6,11]. Note that the argument leading to (2.1) only works for contractible loops, i.e., loops that do not wrap around the periodic direction. To obtain the correct weighing also for non-contractible loops one introduces a vertical seam separating the first and the last vertex in each row [11]. Horizontal edges cutting the seam are assigned an extra weight of a (resp. a^{-1}) when covered by a left-pointing (resp. right-pointing) arrow; the convention does *not* depend on the color of the arrow. Clearly, non-contractible loops can only wind once, so a is fixed by

$$n = a + a^{-1}. \quad (2.2)$$

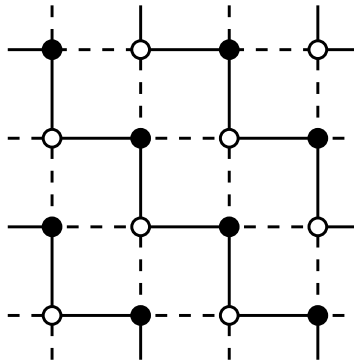


Fig. 2: Parity convention for vertices and edges of the square lattice. Even (resp. odd) edges are shown in dashed (resp. solid) linestyle. Even (resp. odd) vertices are shown as dashed (resp. solid) circles.

With these boundary conditions, the FPL^2 model contains three conserved quantities [11]. To explain these, we shall adopt a convention for the parity of both the vertices and the edges, as shown in Fig. 2. The three components of the conserved charge which are conserved by the evolution along the cylinder are

$$Q = \begin{pmatrix} L \\ L \\ L \end{pmatrix} - \begin{pmatrix} N_{w\downarrow} + N_{eb} \\ N_{\downarrow} \\ N_{w\downarrow} + N_{ob} \end{pmatrix}, \quad (2.3)$$

where N_{\dots} is the number of vertical edges of a given parity ($e = \text{even}$, $o = \text{odd}$) in the concerned row, b (black) or w (white) refers to the color of the arrow, and \uparrow (up) or \downarrow (down) to its orientation. The constant term has been added for convenience. Strictly speaking, it would make better sense to talk about conserved charges with respect to a parity convention for the columns that does not alternate from row to row. In this respect, the charges (2.3) only commute with the transfer matrix that adds *two rows* at a time.

3. The transfer matrix

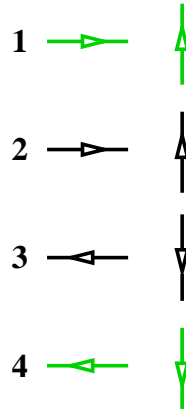


Fig. 3: Convention for the labeling of arrow states on an even edge.

Before going on we shall adopt a convention for labeling the arrow state $i = 1, 2, 3, 4$ of each edge in the FPL^2 model. This is shown in Fig. 3 for the case of an even edge; the convention for an odd edge is similar, but with all arrows reversed (i.e., $i \rightarrow 5 - i$).

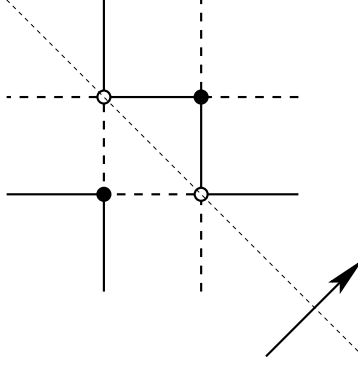


Fig. 4: The FPL^2 model R-matrix adds two even and two odd vertices as shown. The arrow indicates the transfer direction. The parity of vertices and edges follow the conventions of Fig. 2. The four dangling edges below (resp. above) the thin dashed line specify the in-state (resp. the out-state).

We have seen above that from the point of view of the conserved charges, it is most natural to build up the lattice by adding two rows at a time. We have also assumed that the horizontal strip is of even width $2L$. In order to define the row-to-row transfer matrix T , we first define a 256×256 matrix, which we denote, in analogy with integrable models, by R ; it adds four vertices as shown in Fig. 4. Using the weights of Fig. 1, it is straightforward to write R explicitly, in the basis obtained by using the labeling of Fig. 3 for the external lines and by taking the tensor product of the corresponding vector spaces.

The transfer matrix that propagates the system in the upwards direction then reads

$$T = \text{tr}_a R_{aL} \cdots R_{a2} R_{a1} (\Omega^{-1} \otimes \Omega), \quad (3.1)$$

where the subscript a denotes the “auxiliary space” (the pair of horizontal lines) of dimension 16 and the subscripts $1, 2, \dots, L$ correspond to the L pairs of vertical lines which form the “physical space”. The twist $\Omega^{-1} \otimes \Omega$ is a matrix in the auxiliary space which takes care of the effect of the seam; explicitly, $\Omega = \text{diag}(1/a, 1/a, a, a)$ acts on the upper horizontal line whereas Ω^{-1} acts on the lower line.

We now introduce another R-matrix which is related to the affine quantum group $U_q(\widehat{sl(4)})$, where $q = -\omega^{-4}$ (so that $n = -q - q^{-1}$), and which we call \mathbf{R} . It is schematically described by Fig. 5, in which the two representations \square and \boxplus of $U_q(\widehat{sl(4)})$ appear in an alternating fashion. Conventions are such that at a vertex where two lines intersect, the first factor in the tensor product refers to the leftmost line of the in-state, when seen along the transfer direction.

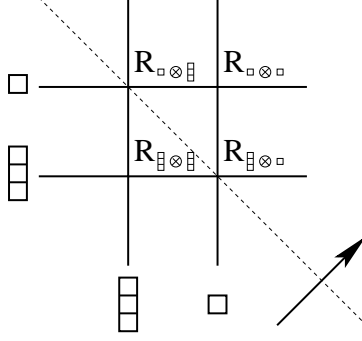


Fig. 5: R-matrix for two rows and two columns, which alternately carry the fundamental representation of $U_q(\widehat{sl(4)})$ and its conjugate. The arrow indicates the transfer direction.

The four R-matrices which appear on Fig. 5 can be expressed as: [12]

$$\check{\mathbf{R}}_{\square \otimes \square}(x) = (qx - q^{-1}x^{-1})\check{\mathbf{P}}_{\square \otimes \square}^{\square \square} + (qx^{-1} - q^{-1}x)\check{\mathbf{P}}_{\square \otimes \square}^{\square \square}, \quad (3.2a)$$

$$\check{\mathbf{R}}_{\square \otimes \square}(x) = (q^2x - q^{-2}x^{-1})\check{\mathbf{P}}_{\square \otimes \square}^{\square \square} + (q^2x^{-1} - q^{-2}x)\check{\mathbf{P}}_{\square \otimes \square}^{\emptyset \square}, \quad (3.2b)$$

$$\check{\mathbf{R}}_{\square \otimes \square}(x) = (q^2x - q^{-2}x^{-1})\check{\mathbf{P}}_{\square \otimes \square}^{\square \square} + (q^2x^{-1} - q^{-2}x)\check{\mathbf{P}}_{\square \otimes \square}^{\emptyset \square}, \quad (3.2c)$$

$$\check{\mathbf{R}}_{\square \otimes \square}(x) = (qx - q^{-1}x^{-1})\check{\mathbf{P}}_{\square \otimes \square}^{\square \square} + (qx^{-1} - q^{-1}x)\check{\mathbf{P}}_{\square \otimes \square}^{\square \square}. \quad (3.2d)$$

We have as usual denoted $\check{\mathbf{R}} \equiv \Pi \mathbf{R}$, where Π is the operator that permutes the two factors of the tensor product. The $\check{\mathbf{P}}$ are intertwining operators which can be computed using representation theory; the parameter x is the ratio of spectral parameters of the horizontal and vertical line. We shall give the explicit matrix representations of the R-matrices below, after fixing the values of x .

In the present context, one can first define separately transfer matrices for even and odd rows (however, only their product will be directly related to the previous transfer matrix T). Indeed, we define $\mathbf{R}_{\square}(x) = \mathbf{R}_{\square \otimes \square}(x/x_{\square})\mathbf{R}_{\square \otimes \square}(x/x_{\square})$ and $\mathbf{R}_{\square}(x) = \mathbf{R}_{\square \otimes \square}(x/x_{\square})\mathbf{R}_{\square \otimes \square}(x/x_{\square})$, where the products are meant as in Fig. 5, and the spectral parameters of vertical lines x_{\square} , x_{\square} are supposed to be fixed. Define next

$$\mathbf{T}_{\square}(x) = \text{tr}_{\square} \mathbf{R}_{\square L}(x) \cdots \mathbf{R}_{\square 2}(x) \mathbf{R}_{\square 1}(x) \Omega^{-1} \quad (3.3a)$$

$$\mathbf{T}_{\square}(x) = \text{tr}_{\square} \mathbf{R}_{\square L}(x) \cdots \mathbf{R}_{\square 2}(x) \mathbf{R}_{\square 1}(x) \Omega \quad (3.3b)$$

where, as before, the indices determine the spaces on which the matrices act. Note that Ω and Ω^{-1} can be considered as the same element of the Cartan subalgebra of $U_q(\widehat{sl(4)})$, but

in fundamental and conjugate representations respectively. Due to the Yang–Baxter equation, the $\mathbf{T}_{\square}(x)$ and $\mathbf{T}_{\square}(x)$ form an infinite family of commuting matrices; their product, the two-row transfer matrix $\mathbf{T}(x, y) = \mathbf{T}_{\square}(x)\mathbf{T}_{\square}(y) = \mathbf{T}_{\square}(y)\mathbf{T}_{\square}(x)$, is itself of the form

$$\mathbf{T}(x, y) = \text{tr}_a \mathbf{R}_{aL}(x, y) \cdots \mathbf{R}_{a2}(x, y) \mathbf{R}_{a1}(x, y) (\Omega^{-1} \otimes \Omega) \quad (3.4)$$

where $\mathbf{R}(x, y) = \mathbf{R}_{\square}(x)\mathbf{R}_{\square}(y)$.

The claim is that the two R-matrices for two rows and two columns R and \mathbf{R} that we have introduced are related. At this point we choose all horizontal lines (whether odd or even) to have the same spectral parameter, and similarly for all vertical lines, so that the ratio is constant and is: $x = q^{-1}$. Note that at this special value, the matrices $\check{\mathbf{R}}_{\square \otimes \square}$ and $\check{\mathbf{R}}_{\square \otimes \square}$ become proportional to projectors onto the antisymmetric sub-representations (this enforces the fact that two loops of the same color cannot cross each other).

Explicitly: ($c = q^{-1} - q$)

$$\check{\mathbf{R}}_{\square \otimes \square}(q) = c \begin{pmatrix} 0 & 0 & 0 & 0 & 0 & 0 & 0 & 0 & 0 & 0 & 0 & 0 & 0 & 0 & 0 & 0 \\ 0 & -q & 0 & 0 & 1 & 0 & 0 & 0 & 0 & 0 & 0 & 0 & 0 & 0 & 0 & 0 \\ 0 & 0 & -q & 0 & 0 & 0 & 0 & 0 & 1 & 0 & 0 & 0 & 0 & 0 & 0 & 0 \\ 0 & 0 & 0 & -q & 0 & 0 & 0 & 0 & 0 & 0 & 0 & 0 & 1 & 0 & 0 & 0 \\ 0 & 1 & 0 & 0 & -q^{-1} & 0 & 0 & 0 & 0 & 0 & 0 & 0 & 0 & 0 & 0 & 0 \\ 0 & 0 & 0 & 0 & 0 & 0 & 0 & 0 & 0 & 0 & 0 & 0 & 0 & 0 & 0 & 0 \\ 0 & 0 & 0 & 0 & 0 & 0 & -q & 0 & 0 & 1 & 0 & 0 & 0 & 0 & 0 & 0 \\ 0 & 0 & 0 & 0 & 0 & 0 & 0 & -q & 0 & 0 & 0 & 0 & 0 & 1 & 0 & 0 \\ 0 & 0 & 1 & 0 & 0 & 0 & 0 & 0 & -q^{-1} & 0 & 0 & 0 & 0 & 0 & 0 & 0 \\ 0 & 0 & 0 & 0 & 0 & 0 & 1 & 0 & 0 & -q^{-1} & 0 & 0 & 0 & 0 & 0 & 0 \\ 0 & 0 & 0 & 0 & 0 & 0 & 0 & 0 & 0 & 0 & 0 & 0 & 0 & 0 & 0 & 0 \\ 0 & 0 & 0 & 0 & 0 & 0 & 0 & 0 & 0 & 0 & -q & 0 & 0 & 1 & 0 & 0 \\ 0 & 0 & 0 & 1 & 0 & 0 & 0 & 0 & 0 & 0 & 0 & -q^{-1} & 0 & 0 & 0 & 0 \\ 0 & 0 & 0 & 0 & 0 & 0 & 0 & 1 & 0 & 0 & 0 & 0 & -q^{-1} & 0 & 0 & 0 \\ 0 & 0 & 0 & 0 & 0 & 0 & 0 & 0 & 0 & 0 & 1 & 0 & 0 & 0 & -q^{-1} & 0 \\ 0 & 0 & 0 & 0 & 0 & 0 & 0 & 0 & 0 & 0 & 0 & 0 & 0 & 0 & 0 & 0 \end{pmatrix} \quad (3.5a)$$

$$\check{\mathbf{R}}_{\square \otimes \square}(q) = c \begin{pmatrix} 0 & 0 & 0 & 0 & 0 & -q & 0 & 0 & 0 & 0 & -q^3 & 0 & 0 & 0 & 0 & -q^5 \\ 0 & 0 & 0 & 0 & 1 & 0 & 0 & 0 & 0 & 0 & 0 & 0 & 0 & 0 & 0 & 0 \\ 0 & 0 & 0 & 0 & 0 & 0 & 0 & 0 & 1 & 0 & 0 & 0 & 0 & 0 & 0 & 0 \\ 0 & 0 & 0 & 0 & 0 & 0 & 0 & 0 & 0 & 0 & 0 & 0 & 1 & 0 & 0 & 0 \\ 0 & 1 & 0 & 0 & 0 & 0 & 0 & 0 & 0 & 0 & 0 & 0 & 0 & 0 & 0 & 0 \\ -q^{-1} & 0 & 0 & 0 & 0 & 0 & 0 & 0 & 0 & 0 & -q & 0 & 0 & 0 & 0 & -q^3 \\ 0 & 0 & 0 & 0 & 0 & 0 & 0 & 0 & 1 & 0 & 0 & 0 & 0 & 0 & 0 & 0 \\ 0 & 0 & 0 & 0 & 0 & 0 & 0 & 0 & 0 & 0 & 0 & 0 & 0 & 1 & 0 & 0 \\ 0 & 0 & 1 & 0 & 0 & 0 & 0 & 0 & 0 & 0 & 0 & 0 & 0 & 0 & 0 & 0 \\ 0 & 0 & 0 & 0 & 0 & 0 & 1 & 0 & 0 & 0 & 0 & 0 & 0 & 0 & 0 & 0 \\ -q^{-3} & 0 & 0 & 0 & 0 & -q^{-1} & 0 & 0 & 0 & 0 & 0 & 0 & 0 & 0 & 0 & -q \\ 0 & 0 & 0 & 0 & 0 & 0 & 0 & 0 & 0 & 0 & 0 & 0 & 0 & 0 & 1 & 0 \\ 0 & 0 & 0 & 1 & 0 & 0 & 0 & 0 & 0 & 0 & 0 & 0 & 0 & 0 & 0 & 0 \\ 0 & 0 & 0 & 0 & 0 & 0 & 0 & 1 & 0 & 0 & 0 & 0 & 0 & 0 & 0 & 0 \\ 0 & 0 & 0 & 0 & 0 & 0 & 0 & 0 & 0 & 0 & 1 & 0 & 0 & 0 & 0 & 0 \\ -q^{-5} & 0 & 0 & 0 & 0 & -q^{-3} & 0 & 0 & 0 & 0 & -q^{-1} & 0 & 0 & 0 & 0 & 0 \end{pmatrix} \quad (3.5b)$$

$$\check{\mathbf{R}}_{\square \otimes \square}(q) = c \begin{pmatrix} 0 & 0 & 0 & 0 & 0 & -q & 0 & 0 & 0 & 0 & -q & 0 & 0 & 0 & 0 & -q \\ 0 & 0 & 0 & 0 & 1 & 0 & 0 & 0 & 0 & 0 & 0 & 0 & 0 & 0 & 0 & 0 \\ 0 & 0 & 0 & 0 & 0 & 0 & 0 & 0 & 0 & 1 & 0 & 0 & 0 & 0 & 0 & 0 \\ 0 & 0 & 0 & 0 & 0 & 0 & 0 & 0 & 0 & 0 & 0 & 0 & 0 & 1 & 0 & 0 \\ 0 & 1 & 0 & 0 & 0 & 0 & 0 & 0 & 0 & 0 & 0 & 0 & 0 & 0 & 0 & 0 \\ -q^{-1} & 0 & 0 & 0 & 0 & 0 & 0 & 0 & 0 & 0 & -q & 0 & 0 & 0 & 0 & -q \\ 0 & 0 & 0 & 0 & 0 & 0 & 0 & 0 & 0 & 1 & 0 & 0 & 0 & 0 & 0 & 0 \\ 0 & 0 & 0 & 0 & 0 & 0 & 0 & 0 & 0 & 0 & 0 & 0 & 0 & 1 & 0 & 0 \\ 0 & 0 & 1 & 0 & 0 & 0 & 0 & 0 & 0 & 0 & 0 & 0 & 0 & 0 & 0 & 0 \\ 0 & 0 & 0 & 0 & 0 & 0 & 1 & 0 & 0 & 0 & 0 & 0 & 0 & 0 & 0 & 0 \\ -q^{-1} & 0 & 0 & 0 & 0 & -q^{-1} & 0 & 0 & 0 & 0 & 0 & 0 & 0 & 0 & 0 & -q \\ 0 & 0 & 0 & 0 & 0 & 0 & 0 & 0 & 0 & 0 & 0 & 0 & 0 & 0 & 1 & 0 \\ 0 & 0 & 0 & 1 & 0 & 0 & 0 & 0 & 0 & 0 & 0 & 0 & 0 & 0 & 0 & 0 \\ 0 & 0 & 0 & 0 & 0 & 0 & 0 & 1 & 0 & 0 & 0 & 0 & 0 & 0 & 0 & 0 \\ -q^{-1} & 0 & 0 & 0 & 0 & -q^{-1} & 0 & 0 & 0 & 0 & -q^{-1} & 1 & 0 & 0 & 0 & 0 \end{pmatrix} \quad (3.5c)$$

$$\check{\mathbf{R}}_{\square \otimes \square}(q) = c \begin{pmatrix} 0 & 0 & 0 & 0 & 0 & 0 & 0 & 0 & 0 & 0 & 0 & 0 & 0 & 0 & 0 & 0 \\ 0 & -q^{-1} & 0 & 0 & 1 & 0 & 0 & 0 & 0 & 0 & 0 & 0 & 0 & 0 & 0 & 0 \\ 0 & 0 & -q^{-1} & 0 & 0 & 0 & 0 & 1 & 0 & 0 & 0 & 0 & 0 & 0 & 0 & 0 \\ 0 & 0 & 0 & -q^{-1} & 0 & 0 & 0 & 0 & 0 & 0 & 0 & 1 & 0 & 0 & 0 & 0 \\ 0 & 1 & 0 & 0 & -q & 0 & 0 & 0 & 0 & 0 & 0 & 0 & 0 & 0 & 0 & 0 \\ 0 & 0 & 0 & 0 & 0 & 0 & 0 & 0 & 0 & 0 & 0 & 0 & 0 & 0 & 0 & 0 \\ 0 & 0 & 0 & 0 & 0 & 0 & -q^{-1} & 0 & 1 & 0 & 0 & 0 & 0 & 0 & 0 & 0 \\ 0 & 0 & 0 & 0 & 0 & 0 & 0 & -q^{-1} & 0 & 0 & 0 & 0 & 1 & 0 & 0 & 0 \\ 0 & 0 & 1 & 0 & 0 & 0 & 0 & 0 & -q & 0 & 0 & 0 & 0 & 0 & 0 & 0 \\ 0 & 0 & 0 & 0 & 0 & 0 & 1 & 0 & 0 & -q & 0 & 0 & 0 & 0 & 0 & 0 \\ 0 & 0 & 0 & 0 & 0 & 0 & 0 & 0 & 0 & 0 & 0 & -q^{-1} & 0 & 0 & 0 & 0 \\ 0 & 0 & 0 & 1 & 0 & 0 & 0 & 0 & 0 & 0 & 0 & 0 & -q & 0 & 0 & 0 \\ 0 & 0 & 0 & 0 & 0 & 0 & 0 & 1 & 0 & 0 & 0 & 0 & 0 & -q & 0 & 0 \\ 0 & 0 & 0 & 0 & 0 & 0 & 0 & 0 & 0 & 0 & 1 & 0 & 0 & 0 & -q & 0 \\ 0 & 0 & 0 & 0 & 0 & 0 & 0 & 0 & 0 & 0 & 0 & 0 & 0 & 0 & 0 & 0 \end{pmatrix} \quad (3.5d)$$

Note that we use the standard bases for \square and \square (which are dual bases of each other).

One can then check that

$$\mathbf{R} = c^4 U R U^{-1} \quad (3.6)$$

where the constant c^4 takes care of the extra factors in Eqs. (3.5), and U is a diagonal matrix that fully factorizes as a tensor product over the four incoming lines: $U = U_{h\square} \otimes U_{h\square} \otimes U_{v\square} \otimes U_{v\square}$, with as a possible choice

$$\begin{aligned} U_{h\square} &= \begin{pmatrix} \omega^6 & 0 & 0 & 0 \\ 0 & \omega^4 & 0 & 0 \\ 0 & 0 & \omega^2 & 0 \\ 0 & 0 & 0 & 1 \end{pmatrix} & U_{h\square} &= \begin{pmatrix} \omega^6 & 0 & 0 & 0 \\ 0 & \omega^4 & 0 & 0 \\ 0 & 0 & \omega^2 & 0 \\ 0 & 0 & 0 & 1 \end{pmatrix} \\ U_{v\square} &= \begin{pmatrix} \omega^{12} & 0 & 0 & 0 \\ 0 & \omega^8 & 0 & 0 \\ 0 & 0 & \omega^4 & 0 \\ 0 & 0 & 0 & 1 \end{pmatrix} & U_{v\square} &= \begin{pmatrix} \omega^{-6} & 0 & 0 & 0 \\ 0 & \omega^{-4} & 0 & 0 \\ 0 & 0 & \omega^{-2} & 0 \\ 0 & 0 & 0 & 1 \end{pmatrix} \end{aligned} \quad (3.7)$$

Consequently, the corresponding transfer matrices T and \mathbf{T} are also similar up to a constant:

$$\mathbf{T} = c^{4L} U_v T U_v^{-1} \quad (3.8)$$

where U_v is the tensor product of $U_{v\square}$ and $U_{v\square}$ for all vertical lines.

$$\begin{aligned}
\langle \downarrow \uparrow \uparrow \downarrow \downarrow | R | \uparrow \downarrow \downarrow \uparrow \rangle &= \begin{array}{c} \begin{array}{c} \downarrow \uparrow \\ \leftarrow \rightarrow \\ \leftarrow \rightarrow \\ \downarrow \uparrow \end{array} \\ \omega^6 \end{array} + \begin{array}{c} \begin{array}{c} \downarrow \uparrow \\ \leftarrow \rightarrow \\ \leftarrow \rightarrow \\ \downarrow \uparrow \end{array} \\ \omega^{-2} \end{array} \\
\langle \uparrow \uparrow \downarrow \downarrow | R | \uparrow \downarrow \uparrow \downarrow \rangle &= \begin{array}{c} \begin{array}{c} \uparrow \uparrow \\ \leftarrow \rightarrow \\ \leftarrow \rightarrow \\ \uparrow \uparrow \end{array} \\ \omega^{-6} \end{array} + \begin{array}{c} \begin{array}{c} \uparrow \uparrow \\ \leftarrow \rightarrow \\ \leftarrow \rightarrow \\ \uparrow \uparrow \end{array} \\ \omega^2 \end{array} \\
\langle \uparrow \downarrow \downarrow \uparrow \downarrow | R | \downarrow \uparrow \uparrow \downarrow \rangle &= \begin{array}{c} \begin{array}{c} \uparrow \downarrow \\ \leftarrow \rightarrow \\ \leftarrow \rightarrow \\ \uparrow \downarrow \end{array} \\ \omega^4 \end{array} + \begin{array}{c} \begin{array}{c} \uparrow \downarrow \\ \leftarrow \rightarrow \\ \leftarrow \rightarrow \\ \uparrow \downarrow \end{array} \\ \omega^{-4} \end{array}
\end{aligned}$$

Fig. 6: Examples of nontrivial R-matrix elements in the FPL^2 model.

Obviously, space does not permit us to reproduce the resulting 256×256 matrices R and \mathbf{R} . Rather, Fig. 6 gives three examples of matrix elements. Note that our convention for the R-matrix (see Fig. 4) is to keep fixed indices for the horizontal and vertical lines. Thus, if the arrow configuration (coded as in Fig. 1) is $\rho_4 \rho_3 \rho_2 \rho_1$ for the out-state (read from left to right when looking along the transfer direction), it is $\rho_2 \rho_1 \rho_4 \rho_3$ for the in-state. The three examples in Fig. 6 then read explicitly: $R_{81,18} = \omega^6 + \omega^{-2}$; $R_{103,91} = \omega^{-6} + \omega^2$; and $R_{239,188} = \omega^4 + \omega^{-4}$. The corresponding entries of \mathbf{R} are found from (3.6).

4. Algebraic Bethe Ansatz

The set of commuting transfer matrices $\mathbf{T}_{\square}(x)$, $\mathbf{T}_{\boxplus}(x)$ can be diagonalized using the so-called nested Bethe Ansatz. We shall not describe this procedure here and refer to [13,14,15] for details. The eigenstates are built by action of operators which depend on parameters that we call $u_k^{(i)}$, with $i = 1, 2, 3$ and $k = 1, \dots, m^{(i)}$, on a reference eigenstate (highest weight state) which has only white arrows pointing up. These parameters satisfy equations, which, in our parameterization, are algebraic in the $e^{i\gamma u_k^{(i)}}$, where γ is such that $q = -e^{-i\gamma}$. Explicitly, call $\omega^{(i)}$ the diagonal elements of the twist Ω in the fundamental

representation (here, $\omega^{(1)} = \omega^{(2)} = 1/a$, $\omega^{(3)} = \omega^{(4)} = a$), with $\prod_{i=1}^4 \omega^{(i)} = 1$; and define the functions $Q^{(i)}(u) = \prod_{k=1}^{m^{(i)}} \sin \gamma(u - u_k^{(i)})$, $i = 1, 2, 3$. $Q^{(0)} \equiv Q^{(4)} \equiv 1$. Then the Bethe Ansatz equations read

$$-\frac{Q^{(i+1)}(u_k^{(i)} + 1) Q^{(i)}(u_k^{(i)} - 1)}{Q^{(i+1)}(u_k^{(i)}) Q^{(i)}(u_k^{(i)} + 1)} \frac{Q^{(i-1)}(u_k^{(i)})}{Q^{(i-1)}(u_k^{(i)} - 1)} = \frac{\omega^{(i)}}{\omega^{(i+1)}} \frac{f^{(i)}(u_k^{(i)})}{f^{(i+1)}(u_k^{(i)})} \quad (4.1)$$

for $1 \leq i \leq 3$, $1 \leq k \leq m^{(i)}$. The functions $f^{(i)}$ depend on the representations and spectral parameters of the physical space (and on the twist); here, one easily computes $f^{(1)}(u) = \omega^{(1)}(\sin \gamma u \sin \gamma(u - 1))^L$, $f^{(i)}(u) = \omega^{(i)}(\sin \gamma(u + 1) \sin \gamma(u - 1))^L$ for $i = 2, 3$, $f^{(4)}(u) = \omega^{(4)}(\sin \gamma(u + 1) \sin \gamma u)^L$.

The corresponding eigenvalues of $\mathbf{T}_{\square}(u)$ and $\mathbf{T}_{\square}(u)$, in the parameterization $x = -e^{i\gamma(u+1)}$, are

$$t_{\square}(u) = X^{(1)}(u) + X^{(2)}(u) + X^{(3)}(u) + X^{(4)}(u) \quad (4.2a)$$

$$t_{\square}(u) = \tilde{X}^{(1)}(u) + \tilde{X}^{(2)}(u) + \tilde{X}^{(3)}(u) + \tilde{X}^{(4)}(u) \quad (4.2b)$$

where $X^{(i)}(u) = \frac{Q^{(i-1)}(u-1)}{Q^{(i-1)}(u)} \frac{Q^{(i)}(u+1)}{Q^{(i)}(u)} f^{(i)}(u)$ and $\tilde{X}^{(i)}(u) = \frac{Q^{(i-1)}(u+i-2)}{Q^{(i-1)}(u+i-3)} \frac{Q^{(i)}(u+i-3)}{Q^{(i)}(u+i-2)} f^{(5-i)}(u)$.

We now choose $u = 0$, so that the $X^{(1)}$, $X^{(4)}$, $\tilde{X}^{(1)}$, $\tilde{X}^{(4)}$ vanish (this, once again, can be interpreted as a consequence of the requirement that two loops of the same color do not cross each other). Finally, we consider the two row-matrix $\mathbf{T} = \mathbf{T}_{\square} \mathbf{T}_{\square}$. Its eigenvalue is obtained by taking the product of the remaining terms in Eqs. (4.2); rewriting the $X^{(i)}$ as functions of $Q^{(i)}$, getting rid of the extra factors $\sin \gamma$ which compensate the factors of c in Eq. (3.8), we find the eigenvalues of T to be

$$\begin{aligned} t &= 2 \frac{Q^{(2)}(1)Q^{(2)}(-1)}{Q^{(2)}(0)^2} + \frac{\omega^{(2)}}{\omega^{(3)}} \left(\frac{Q^{(2)}(1)}{Q^{(2)}(0)} \right)^2 \frac{Q^{(1)}(-1)}{Q^{(1)}(0)} \frac{Q^{(3)}(0)}{Q^{(3)}(1)} + \frac{\omega^{(3)}}{\omega^{(2)}} \left(\frac{Q^{(2)}(-1)}{Q^{(2)}(0)} \right)^2 \frac{Q^{(1)}(0)}{Q^{(1)}(-1)} \frac{Q^{(3)}(1)}{Q^{(3)}(0)} \\ &= \left(a^{-1} \frac{Q^{(2)}(1)}{Q^{(2)}(0)} \sqrt{\frac{Q^{(1)}(-1)}{Q^{(1)}(0)} \frac{Q^{(3)}(0)}{Q^{(3)}(1)}} + a \frac{Q^{(2)}(-1)}{Q^{(2)}(0)} \sqrt{\frac{Q^{(1)}(0)}{Q^{(1)}(-1)} \frac{Q^{(3)}(1)}{Q^{(3)}(0)}} \right)^2 \end{aligned} \quad (4.3)$$

where in the last line we have used the explicit expression of the twist. This is precisely the square of the expression found in [11] for the one-row transfer matrix. The correspondence of notations is as follows:

$$u_k \equiv 2i(u_k^{(1)} + 1/2) \quad v_k \equiv 2i(u_k^{(3)} - 1/2) \quad w_k \equiv 2iu_k^{(2)} \quad (4.4)$$

Furthermore, the Cartan subalgebra produces three conserved quantities; in fundamental and conjugate representations, they have the following expression: (basis of the dual of the root lattice)

$$\left. \begin{matrix} Q_{1\blacksquare} \\ -Q_{1\blacksquare} \end{matrix} \right\} = \begin{pmatrix} 1 & 0 & 0 & 0 \\ 0 & 0 & 0 & 0 \\ 0 & 0 & 0 & 0 \\ 0 & 0 & 0 & 0 \end{pmatrix} - \frac{1}{4}I \quad \left. \begin{matrix} Q_{2\blacksquare} \\ -Q_{2\blacksquare} \end{matrix} \right\} = \begin{pmatrix} 1 & 0 & 0 & 0 \\ 0 & 1 & 0 & 0 \\ 0 & 0 & 0 & 0 \\ 0 & 0 & 0 & 0 \end{pmatrix} - \frac{1}{2}I \quad \left. \begin{matrix} Q_{3\blacksquare} \\ -Q_{3\blacksquare} \end{matrix} \right\} = \begin{pmatrix} 1 & 0 & 0 & 0 \\ 0 & 1 & 0 & 0 \\ 0 & 0 & 1 & 0 \\ 0 & 0 & 0 & 0 \end{pmatrix} - \frac{3}{4}I \quad (4.5)$$

Combining this with the correspondence given by Fig. 3, it is easy to identify them with the components of the charge Q of Eq. (2.3). Their value is determined by the numbers $m^{(i)}$ of Bethe roots of kind i : each root of the kind i decreases by one the i^{th} component of the charge, starting from the reference state which has $Q = \begin{pmatrix} L \\ L \\ L \end{pmatrix}$. Comparing with Eq. (2.3), we deduce that

$$m^{(1)} = N_{w\downarrow} + N_{eb} \quad m^{(2)} = N_{\downarrow} \quad m^{(3)} = N_{w\downarrow} + N_{ob} \quad (4.6)$$

Note that if $m^{(1)} > 0$ but $m^{(3)} = 0$, only even arrows are modified compared to the reference state (i.e. all odd arrows are white pointing up); and similarly for $m^{(3)} > 0$, $m^{(1)} = 0$ and odd arrows.

5. Results and conclusions

We have found that the nested algebraic Bethe Ansatz can be used to solve the FPL² model at $n_b = n_w$. The latter is therefore identified with a standard integrable vertex model associated to $U_q(\widehat{sl(4)})$, and its transfer matrix embedded into an infinite set of commuting transfer matrices; and many results follow immediately.

In particular, the long distance behavior of this type of models has been studied by many methods (see for instance [16,17,18]). For $|n| > 2$ the spectrum has a gap and the correlation length is finite. In the following we focus instead on the critical regime $|n| \leq 2$, and we parameterize $n = 2 \cos \gamma$.

As our model is isotropic, we expect the largest eigenvalue of the transfer matrix to have the following asymptotic behavior [19]

$$\log t_0(L) = -L f_0 + \frac{\pi c}{6L} + \dots \quad \text{for } L \rightarrow \infty, \quad (5.1)$$

where c is the central charge of the infra-red conformal field theory. Here note that only fundamental representations (\square and \blacksquare) are used, so we are dealing with a non-fused model. Assuming the usual form for the ground state, standard computations (see e.g. [18]) lead, in this type of models, to the following form of c

$$c = r - \frac{3}{\pi(\pi - \gamma)} \langle w | C^{-1} | w \rangle \quad (5.2)$$

where r and C are respectively the rank and the Cartan matrix of the underlying algebra, and w is a vector with components $w_s = \frac{1}{i} \log(\omega^{(s)}/\omega^{(s+1)})$ that parameterizes the twist. If we now specialize to A_3 and to our choice of boundary conditions: $w_1 = w_3 = 0$, $w_2 = -2\gamma$, we obtain

$$c = 3 - 12 \frac{\gamma^2}{\pi(\pi - \gamma)}, \quad (5.3)$$

which coincides with what was found in [4]. Note that this is not the central charge of the $W(A_3)$ conformal field theory—the latter can also be obtained within the framework of this model, but with a different twist.

One can also investigate the nature of excitations above the ground state. They are, of course, gapless and describe solitons associated to the three fundamental representations of A_3 interacting with the standard S-matrices [18,20], plus possible bound states in certain regimes of γ . In the infra-red limit the dispersion relation can be linearized and the corresponding low-lying excited states are related to the conformal weights Δ_n of the aforementioned CFT via

$$\log t_n(L) = -L f_0 + \frac{\pi(c - 24\Delta_n)}{6L} + \dots \quad \text{for } L \rightarrow \infty. \quad (5.4)$$

One can check that the weights thus obtained fit with the formulae of the Coulomb gas picture:

$$\Delta_n = \frac{1}{4} \langle e | K^{-1} | e - 2e_0 \rangle + \frac{1}{4} \langle m | K | m \rangle \quad (5.5)$$

where $K = \frac{1}{2}(1 - \gamma/\pi)C$, e (resp. m) is the electric (resp. magnetic) charge which belongs to the lattices of weights (resp. roots) of A_3 , and e_0 is the background charge, related to our twist by $e_0 = \frac{1}{2\pi}w$. This constitutes a confirmation of the results of [5]. Incidentally, the fact that for $n_b \neq n_w$ the quadratic form K appearing in the conformal weights as given in [5] is generically not related to a Cartan matrix can be considered an indication of the non-integrability of the model.

We have made some numerical checks of the structure of the ground state and excited state described above. As it turned out, this picture was confirmed for $n \geq 0$; however, for $n < 0$ the ground state of the usual form (with, using the notations of Eq. (4.4), real u_k, v_k, w_k) is *not* the state corresponding to the dominant eigenvalue of the transfer matrix. Indeed, we have found a $n \rightarrow -n$ symmetry of the eigenvalue spectrum corresponding to the sectors where both $L - m^{(2)}$ and $m^{(1)} + m^{(3)}$ are even, cf. Eq. (4.6); this applies thus in particular to the ground state sector which has $m^{(1)} = m^{(2)} = m^{(3)} = L$. This symmetry can be described in the Bethe Ansatz equations as the transformation of the Bethe roots (with the notations of Eq. (4.4)):

$$\gamma u_k \rightarrow -(\pi - \gamma)u_k \quad \gamma v_k \rightarrow -(\pi - \gamma)v_k \quad \gamma w_k \rightarrow -(\pi - \gamma)w_k + i\pi, \quad (5.6)$$

where we recall that $n = 2 \cos \gamma$, so that $-n = 2 \cos(\pi - \gamma)$. One can check that this transformation leaves the eigenvalues (4.3) invariant. In particular, we conclude that the “real” ground state eigenvalue t_0 only depends on $|n|$, and identifies with the one described above only for $n \geq 0$. For $n < 0$, the “fake” ground state eigenvalue corresponds to a state very high above the real ground state (even the bulk part being different as $L \rightarrow \infty$), whose only special property is that it is the analytic continuation of the $n > 0$ ground state eigenvalue. At the moment, we do not have a satisfactory explanation of this phenomenon. The non-unitarity of the $n < 0$ theory, or our boundary conditions (we can only consider the theory on a cylinder, but not on a torus due to the issue of winding loops) might play some role in it.

[We remark parenthetically that the symmetry of the ground state sector holds true more generally for the $n_b \neq n_w$ FPL² model, under the transformation $(n_b, n_w) \rightarrow (-n_b, -n_w)$. This is based on the observation that, with suitable periodic boundary conditions, all terms in the high-fugacity expansion of the partition function have $N_b + N_w$ even, where N_b (resp. N_w) is the number of black (resp. white) loops. To see this, represent the dominant state at $n_b, n_w \rightarrow \infty$ as an “ideal state” in the four-coloring picture [1], with black (resp. white) loops being an alternation of colors 1 and 2 (resp. 3 and 4). Note that the high-fugacity expansion of the 1–2 (black) and 3–4 (white) loops (disregarding their orientation) can be obtained by only permuting the colors around the two *other* types of small loops (say, of types 1–3 and 2–4), and that these loops stay of length four. Examining all possible 1–2 and 3–4 loop environments of a plaquette occupied by the 1–3 and 2–4 loops proves our statement.]

It is interesting to compare our results with the work of Reshetikhin [21] on fully-packed loops on the hexagonal lattice. After contracting the vertices of the hexagonal lattice two by two, so as to form a square lattice, this author identified the R-matrix with that of the integrable model $U_q(\widehat{sl(3)})$. The choice of spectral parameter, as in our case, makes $\check{\mathbf{R}}$ degenerate into a projection operator. However, there are important differences. First, in [21] the underlying algebra is of course different and all horizontal and vertical lines carry the same representation \square of $U_q(\widehat{sl(3)})$, in contrast to the alternation of \square and \boxplus used here. Second, in [21] there is no twist Ω in the auxiliary space, whence contractible and non-contractible loops carry respective weights of n and 2 . In particular, for $n \leq 2$, the central charge is constant, $c = 2$. When $n = 2$, the continuum limit of the hexagonal-lattice loop model becomes a $SU(3)_{k=1}$ free field Wess-Zumino-Witten theory; this is a consequence of the $U_q(\widehat{sl(3)})$ identification and of the fact that only the fundamental representation is used. Likewise, the $U_q(\widehat{sl(4)})$ identification of the FPL² model reported in the present work implies that the $n = 2$ case is a $SU(4)_{k=1}$ WZW theory in the continuum limit. Indeed, the four-coloring model was originally constructed by Read [2] so as to have a $SU(4)_{k=1}$ symmetry.

References

- [1] J. Kondev and C.L. Henley, *Four-coloring model on the square lattice—a critical ground state*, Phys. Rev. B **52**, 6628–6639 (1995).
- [2] N. Read in *Proceedings of the Kagomé Workshop*, ed. P. Chandra (NEC Laboratories, Princeton, 1992).
- [3] R. Raghavan, C.L. Henley and S.L. Arouh, *New two-color dimer models with critical ground states*, J. Stat. Phys. **86**, 517–550 (1997) (cond-mat/9606220).
- [4] J. Kondev, *Liouville field theory of fluctuating loops*, Phys. Rev. Lett. **78**, 4320–4323 (1997) (cond-mat/9703113).
- [5] J. Kondev and J.L. Jacobsen, *Conformational entropy of compact polymers*, Phys. Rev. Lett. **81**, 2922–2925 (1998) (cond-mat/9805178).
- [6] J.L. Jacobsen and J. Kondev, *Field theory of compact polymers on the square lattice*, Nucl. Phys. B **532**, 635–688 (1998) (cond-mat/9804048).
- [7] J.L. Jacobsen and J. Kondev, *Conformal field theory of the Flory model of protein melting*, preprint (cond-mat/0209247).
- [8] J.L. Jacobsen and J. Kondev, *Continuous melting of compact polymers*, preprint (cond-mat/0401504).
- [9] M.T. Batchelor, H.W.J. Blöte, B. Nienhuis and C.M. Yang, *Critical behaviour of the fully packed loop model on the square lattice*, J. Phys. A **29**, L399–L404 (1996).
- [10] B. Nienhuis, *Tiles and colors*, J. Stat. Phys. **102**, 981–996 (2001) (cond-mat/0005274).
- [11] D. Dei Cont and B. Nienhuis, *The packing of two species of polygons on the square lattice* (cond-mat/0311244).
- [12] G.W. Delius, M.D. Gould and Y.-Z. Zhang, *On the construction of trigonometric solutions of the Yang-Baxter equations*, Nucl. Phys. B **432**, 377–403 (1994) (hep-th/9405030).
- [13] O. Babelon, H.J. de Vega and C.-M. Viallet, Nucl. Phys. B **200**, 266 (1982).
- [14] P.P. Kulish and N.Yu. Reshetikhin, *Diagonalisation of $GL(N)$ invariant transfer matrices and quantum N -wave system (Lee model)*, J. Phys. A **16**, L591 (1983).
- [15] V.V. Bazhanov and N.Yu. Reshetikhin, *Restricted solid-on-solid models connected with simply laced algebras and conformal field theory*, J. Phys. A **23**, 1477 (1990).
- [16] H. de Vega, *Finite-size corrections for nested Bethe Ansatz models and conformal invariance*, J. Phys. A **20**, 6023 (1987); *Integrable vertex models and extended conformal invariance*, J. Phys. A **21**, L1089 (1988).
- [17] Y. Zhou and P. Pearce, *Solution of functional equations of restricted $A_{n-1}^{(1)}$ fused lattice models*, Nucl. Phys. B **446**, 485–510 (1995).
- [18] P. Zinn-Justin, *Non-linear integral equations for complex affine Toda associated to simply laced Lie algebras*, J. Phys. A **31**, 6747 (1998) (hep-th/9712222).

- [19] H. W. J. Blöte, J. L. Cardy and M. P. Nightingale, *Conformal invariance, the central charge, and universal finite-size amplitudes at criticality*, Phys. Rev. Lett. **56**, 742 (1986); I. Affleck, *Universal term in the free energy at a critical point and the conformal anomaly*, Phys. Rev. Lett. **56**, 746 (1986).
- [20] T.J. Hollowood, *Int. J. Mod. Phys. A* **8** (1993), 947.
- [21] N.Y. Reshetikhin, *A new exactly solvable case of an $O(n)$ model on a hexagonal lattice*, J. Phys. A **24**, 2387–2396 (1991).